

Multiobjective Optimization of Integration of the Trombe Wall in Buildings Using a Full Factorial Experiment

K. A. Samiev^{a, *}, A. S. Halimov^a, and Sh. Sh. Fayziev^b

^a Physical-Technical Institute, Academy of Sciences of the Republic of Uzbekistan, Tashkent, 100084 Uzbekistan

^b Bukhara State University, Bukhara, 200114 Uzbekistan

*e-mail: skamoliddin@gmail.com

Received January 6, 2022; revised February 2, 2022; accepted February 27, 2022

Abstract—This paper presents the results of a multiobjective optimization of integration of the Trombe wall in a typical residential building in Uzbekistan using a full factorial experiment. The following parameters were used as factors of the experiment: orientation of the southern wall of a typical building, thermal resistance of translucent fences, ratio of the surface area of the thrombus wall to the surface area of the building façade, and air flow rate through the Trombe wall. Calculations were made for the building with three levels of thermal protection under climate conditions of the city of Tashkent (Uzbekistan). The study object was a typical one-story three-room residential building. It has been revealed that the relative dominance of the factors within the studied range of factor values during the heating period is in the following order: orientation of the southern wall of the building, 4.56%; thermal resistance of translucent fencing, 58.21%; ratio of the surface area of the Trombe wall to the surface area of the building facade, 20.11%, and air flow rate through the Trombe wall, 17.12%. On average, the optimal combination of factors makes it possible to save from 11.1–23.5 to 68.1–93.7% of the annual specific energy consumption of the building during the heating period. Reductions in CO₂ emissions with the use of coal for building heating range from 2106 to 129 731 kg per year. Depending on the investment, the simplified payback period for the integration of the Trombe wall is 12.279 to 28.445 years. Regression equations are proposed for three levels of thermal protection of the study object, which makes it possible to determine the specific energy consumption for heating.

Keywords: solar energy, stationary heat transfer model, Trombe wall system, factorial experiment, multiobjective optimization

DOI: 10.3103/S0003701X22010169

INTRODUCTION

In 2018, the proportion of energy consumption in buildings in Uzbekistan was about 40% of the country's total energy balance; the average value of this indicator throughout the world is 20% [1]. By 2050, the area of housing stock is expected to increase to 949–987 million m² in Uzbekistan. In turn, this leads to an increase in energy consumption in buildings, since about 70% of energy consumed in residential buildings is spent on heat loads during the heating period [2]. In this regard, attention at the national level is paid to addressing these issues in Uzbekistan, including the mandatory use of energy-saving technologies in the construction of all types of buildings since 2020 [3], as well as amendments of some building codes and rules since that time [4–8]. On the other hand, Uzbekistan has a huge potential for using renewable energy sources, which is estimated at about 51 billion TOE; 97% of the renewable energy potential comes from solar energy [2].

Energy consumption can be reduced at the building design stage, taking into account the full load on heating and cooling [9], by optimizing the geometric and thermal parameters of building fences [10], and using methods of passive solar heating systems [11]. The use of passive solar heating methods will reduce heat loads for cooling and heating by up to 54 and 87%, respectively [12]. A way to partially solve this problem is the use of passive solar heating systems with the Trombe wall [13].

The Trombe wall was first developed by Edward Morse in the United States in the 19th century [14] and later improved by French engineer Felix Trombe and architect Jacques Michel [15]. The Trombe wall consists of a translucent barrier, a ventilated or non-ventilated air gap, and a wall made of various materials (brickwork, concrete, etc.), which has a high heat capacity and an outer blackened surface. The Trombe wall is installed with orientation to the south in the northern hemispheres and to the north in the southern hemispheres to produce maximum solar radiation.

The principle of operation of the Trombe wall is as follows: the sun's rays falling on the front surface of translucent fencing are partially reflected, partially absorbed, and partially transmitted. The transmitted sun rays fall on the wall surface and are absorbed. As a result, the temperature of the wall rises and the heat is transferred to the indoor air. It should be noted that the Trombe wall is differently termed in different sources, e.g., the Trombe–Michel wall, solar wall, heat-accumulating wall, accumulating collector wall, or simply accumulating wall [13].

Different modifications of the Trombe wall have been proposed to date [16, 17]: classical Trombe wall; Trombe composite wall, Trombe wall made of phase change material, Trombe photovoltaic wall, Trombe water wall, fluidized bed Trombe wall, air purifying Trombe wall, electrochromic Trombe wall, and translucent insulation Trombe wall. Analysis shows that the number of scientific articles on Trombe wall variants published in different databases (Science Direct, Springer Link, Taylor & Francis Online, SAGE Journals, Wiley Online Library, and MDPI) has increased in recent years (e.g., by 10 times in 2019 compared to 2001) [13].

An energy and exergy analysis was used to study the effect of different factors on the thermal efficiency of the Trombe wall. An increase of parameters, such as the air channel thickness and intensity of solar radiation, to a certain level positively influences the operation of the system. It should be noted that reducing the radiating capacity of glass coating is an effective method for increasing the energy and exergy efficiency [18]. Thermal characteristics of the Trombe wall were analytically and experimentally analyzed for different operating conditions of the ventilation holes and occlusion device. The experimental analysis made it possible to determine temperature fluctuations, the heat flow, thermal delay, and air velocity near the vents. The experimental results showed the possibility of increasing the maximum value of the temperature of the outer surface of the massive wall by about 75% under similar outdoor conditions without using the external occlusion device. At the same time, this led to an increase in the internal temperature by 61%. The values of the temperature of the outer surface of the massive wall exceeded 60°C without the occlusion device, while they decreased to 30°C or lower with the installation of this device [19].

The use of the life cycle cost (LCC) method revealed that the thermally and economically optimal ratio of the surface area of the Trombe wall was 37%. This optimal ratio reduced the LCC by 2.4% and annual CO₂ emissions to 445 kg [20].

The introduction of a thermal fin on the Trombe wall contributes to an increase in the indoor temperature and a decrease in the temperature of the outer surface of the Trombe wall. This leads to a significant increase in the thermal efficiency of this solar system

compared to the same environment without thermal fins [21]. Numerical simulation shows that the 0.08-m-thick heat-storage wall made of hydrated CaCl₂·6H₂O salt maintained a temperature close to the comfort temperature with the lowest indoor fluctuations in indoor temperature compared to the 0.02-m-thick concrete wall and 0.05-m-thick paraffin wall. It was determined that the indoor temperature varied from 18 to 22°C for the wall made of hydrated salt compared to 15–25°C for the other two types. Accordingly, it is recommended to use this material to accumulate heat for passive solar heating in modern buildings [22].

There are studies on passive solar heating systems under climate conditions of Uzbekistan and Turkmenistan. A mathematical model of the indoor thermal regime using passive solar heating systems with three-layer ventilated translucent barriers has been developed [23]. An effect of the indicators of heat resistance and thermal efficiency of a residential building with the Trombe wall and Trombe wall combined with heat pipes has been studied [24, 25]. Coefficients of fuel replacement have been determined in passive solar heating systems with a heat storage wall and three-layer translucent barriers [26, 27].

It should be noted that due attention has not been paid to studies on multiobjective optimization of integration of the Trombe wall in buildings under climate conditions of Uzbekistan. In this study, we used the method of a full factorial experiment for the multiobjective optimization of integration of the Trombe wall in buildings. This method made it possible to find the experimental factors that most significantly influence the thermal characteristics of the building. In this regard, the study also considered the influence of the orientation of the southern wall of the building, influence of the ratio of the surface area of the Trombe wall to the surface area of the building facade, effect of thermal resistance of translucent fencing, and effect of the air flow rate through the Trombe wall on a number of parameters, such as the specific heat consumption of the building, reduction of CO₂ emissions into the atmosphere, and simplified and discounted payback period.

METHODS AND MATERIALS

Energy analysis. The required thermal energy for the needs of building heating during the heating period, taking into account the heating of the ventilation air norm, Q_h^v , is determined by formula [28, 29]:

$$Q_h^v = [Q_h - (\Delta Q + Q_{\text{gain}}) v \xi] \beta_h, \quad (1)$$

where Q_h is the total heat loss of the building during the heating period, kWh; ΔQ is the reduction of the heat loss of the building when the Trombe wall is used, kWh; Q_{gain} is the heat gain from the ventilated Trombe wall, kWh; v is the coefficient of heat gain reduction

due to the thermal inertia of fences; is the efficiency coefficient of the automatic control of heat supply to heating systems; and β_h is the coefficient of additional heat consumption of the heating system.

The total heat loss of the building during the heating period [28] is

$$Q_h = U_{tot} HDD A_{e.sum}, \quad (2)$$

where U_{tot} is the total heat transfer coefficient of the building, $W/(m^2 \text{ } ^\circ C)$; HDD is the number of degree-days of the heating period, degree days; and $A_{e.sum}$ is the total area of the external fences of the heated part of the building, m^2 . The total heat transfer coefficient of the building is calculated as the sum of the transmission (U_{tr}) and infiltration (U_{inf}) heat transfer coefficients

$$U_{tot} = U_{tr} + U_{inf}. \quad (3)$$

The transmission heat transfer coefficient of the building is determined by equation

$$U_{tr} = (U_{wall} A_{wall} + U_c A_c + U_f A_f + U_w A_w + U_{ed} A_{ed}) / A_{e.sum}, \quad (4)$$

where U_{wall} , U_c , U_f , U_w , and U_{ed} are the heat transfer coefficients for the walls, ceilings, floors, windows, and entrance doors of the building, respectively, $W/(m^2 \text{ } ^\circ C)$; A_{wall} , A_c , A_f , A_w , and A_{ed} are the areas of the outer surface of the walls, ceilings, floors, windows, and entrance doors of the building, respectively, m^2 .

$$U_{inf} = c \rho n_a V, \quad (5)$$

where c is the specific heat of indoor air, $J/(kg \text{ } ^\circ C)$; ρ is the density of indoor air, kg/m^3 ; V is the heated volume of the building, m^3 ; and n_a is the air exchange rate, $1/s$.

The total heat loss of the building with the Trombe wall during the heating period is as follows:

$$Q_{h.sw} = U_{tot.sw} HDD A_{e.sum}, \quad (6)$$

The total heat transfer coefficient and transmission heat transfer coefficient of the building with the Trombe wall is determined by the following equation:

$$U_{tot.sw} = U_{tr.sw} + U_{inf}, \quad (7)$$

$$U_{tr.sw} = (U_{wall} A_{wall} + U_c A_c + U_f A_f + U_w A_w + U_{ed} A_{ed} + U_{sw} A_{sw}) / A_{e.sum}, \quad (8)$$

where A_{sw} is the surface area of the Trombe wall, m^2 ; U_{sw} is the heat transfer coefficient through the Trombe wall, $W/(m^2 \text{ } ^\circ C)$;

$$U_{sw} = U_o + \rho c q_{v.sw} \frac{1}{A_{sw}} \frac{U_o^2}{U_i^2} \delta k_{sw}, \quad (9)$$

where U_o is the overall heat transfer coefficient of the Trombe wall, $W/(m^2 \text{ } K)$; $q_{v.sw}$ is the air flow rate through the ventilated layer, m^3/s ; U_i is the coefficient of thermal conductivity of the massive wall, $W/(m^2 \text{ } K)$; and k_{sw} is the dimensionless parameter related to the air layer temperature.

The reduction of heat loss ΔQ based on the use of the Trombe wall alone in the building structure is

$$\Delta Q = Q_h - Q_{h.sw}. \quad (10)$$

According to [30, 31], the heat input from the ventilated Trombe wall during the heating period is

$$Q_{gain} = I_w A_{sw} \alpha_{solw} F_S F_F F_W \times \left[U_o (R_e + R_i) + R_i \frac{U_o^2}{U_i U_e} \frac{\rho_a C_a q_{v.sw}}{A_{sw}} k_{sw} \omega \right], \quad (11)$$

where I_w is the total solar radiation for the heating calculation period, kWh/m^2 ; α_{sol} is the coefficient of solar absorption of the outer surface of the massive wall; F_F is the frame reduction coefficient; F_S is the

shading reduction factor; F_W is the correction factor for nondiffusing glasses; τ_w is the total coefficient of transmittance of solar radiation by the translucent fence; R_e is the thermal resistance of the translucent fence between the air layer and outside environment, $m^2 \text{ } K/W$; R_i is the thermal resistance of the massive wall between the air layer and indoor air, $m^2 \text{ } K/W$; R_l is the thermal resistance of the air layer, $m^2 \text{ } K/W$; and U_e is the heat transfer coefficient of the translucent fence, $W/(m^2 \text{ } K)$.

Economic analysis. The annual capital saving, S , is determined from the following equation

$$S = \frac{(Q_h - Q_h^y) P_d}{g_u \eta_u}, \quad (12)$$

where P_d is the fuel cost, USD; g_u is the specific calorific value of fuel, kWh/kg ; and η_u is the efficiency of the heat source.

The simplified payback period is

$$SPP = \frac{C_{TW}}{S}. \quad (13)$$

The discounted payback period, DPP, is determined by the following equation [10]:

Table 1. Characteristics of double glasses

No.	Glazing variants	Total coefficient of solar energy transmittance	Reduced resistance to heat transfer, m ² °C/W	Cost, USD*, CTW ₀
1	4M1-8-4M1	0.78	0.28	60.50
2	4M1-16-4M1	0.78	0.32	61.75
3	4M1- Ar16-4M1	0.78	0.34	62.40
4	4M1-8-K4	0.76	0.47	66.60
5	4M1-10-K4	0.76	0.49	67.20
6	4M1-16-K4	0.76	0.53	68.44
7	4M1-Ar10-K4	0.76	0.55	69.08
8	4M1-Ar16-K4	0.76	0.59	70.40
9	4M1-Ar10-I4	0.51	0.60	70.70
10	4M1-Ar12-I4	0.51	0.63	71.60
11	4M1-Ar16-I4	0.51	0.66	72.60
12	4M1-Ar12-4M1-Ar12-K4	0.72	0.68	73.22
13	4M1-Ar16-4M1-Ar16-K4	0.72	0.72	74.50

*The cost of double-glasses was chosen based on the data given in [34] using the regression method.

$$DPP = \frac{\ln \left[\left(1 - \frac{rC_{TW}}{S} \right)^{-1} \right]}{\ln(1+r)}, \quad (14)$$

where C_{TW} is the initial investment (cost of the Trombe wall), USD.

$$C_{TW} = ARA_{wall}C_{TW0}, \quad (15)$$

where C_{TW0} is determined from Table 1.

The discount factor (DF) depends on inflation rate g and interest rate i and is determined (according to [30]) as:

$$DF = \frac{(1+r)^{LC} - 1}{r(1+r)^{LC}} \times \begin{cases} r = \frac{i-g}{1+g}, & \text{at } i > g \\ r = \frac{g-i}{1+i}, & \text{at } g > i \end{cases} \quad \text{at } i \neq r, \quad (16)$$

where i is the inflation rate; g is the base rate; if $i = g$, the discount factor is determined as follows:

$$DF = \frac{LC}{1+i}, \quad (17)$$

where LC is the life cycle, years.

Ecological analysis. The amount of CO₂ emission reduction per year can be calculated by the formula [31]:

$$M_{CO_2} = \frac{Q_h - Q_h^y}{g_u \eta_u} F_{CO_2} \frac{44}{12}, \quad (18)$$

where M_{CO_2} is the amount of CO₂ reduction with the use of the Trombe wall instead of the conventional wall

in the life cycle; F_{CO_2} is the factor of carbon emission from different energy sources.

Descriptions of the Study Object

The study object was a typical three-room residential building (Fig. 1). The geometric parameters of the residential building are given in Table 2. A ventilated

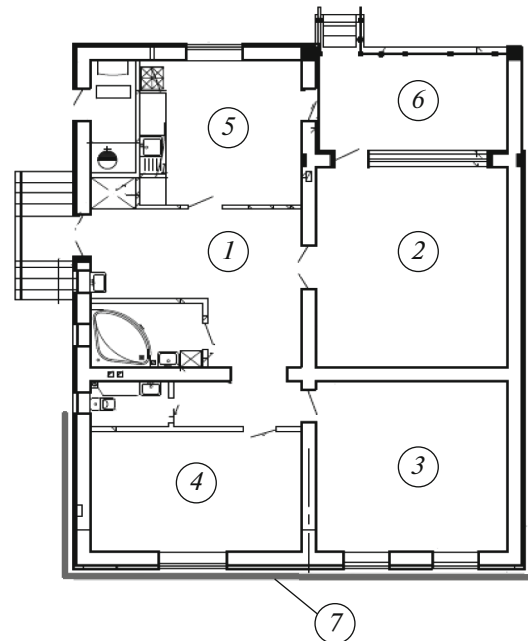


Fig. 1. Typical three-room residential building. (1) Entrance hall; (2) common room; (3) parents' bedroom; (4) bedroom; (5) kitchen; (6) iwan; (7) Trombe wall.

Table 2. Geometric dimensions of the three-room residential building

No	Parameter	Designation and units of measurement	Design value
1.	Area of residential premises	A_c, m^2	126.3
2.	Heated volume	V_h, m^3	381.4
3.	Total area of external building fences	A_c^{sum}, m^2	417.08
4.	including:		
	facades	A_{wall}, m^2	140
	windows and balcony doors	A_w, m^2	19
	entrance doors	A_{ed}, m^2	2.54
	attics	A_{att}	199.28

Trombe wall is installed on the external walls of the building [11]. Different double glasses were used as a translucent part of the Trombe wall; their characteristics are given in Table 1 [33, 34].

CALCULATION METHOD

The rational values of the parameters of the Trombe wall were determined according to a four-factor scheme presented in Table 3. Calculations were made using the method of a factorial experiment, i.e., method of full factorial experiment [35]. Calculations were based on the values presented in Table 4 [30, 36–38]. The cost of stone coal for the design period is 674100 UZS/t (October 11–15, 2021, USD exchange rate 10700.03 UZS) [39, 40].

Model Validation

The formula (11) for the Trombe wall was verified (validated) by comparing the results given in [41, 42]. As follows from Table 5, the root means square (rms) error is 0.047 kWh, rms error in percentage is 8.876%, and the square of the correlation coefficient is $R^2 = 0.765$.

The results of the determination of the specific energy consumption of the building for heating were compared with the data presented in [43]. Comparisons showed that the relative error between the results given in [43] and results of this research is 0.4–1.5%.

RESULTS AND DISCUSSION

For calculations, we developed a computer software program using Python for determining the spe-

Table 3. Test factors and corresponding levels

Levels	Factors			
	building orientation (BO), deg	area ratio (AR)	reduced heat transfer resistance $R_{ce.sum}$, $(m^2 \cdot ^\circ C)/W$	air flow rate through the Trombe wall, m^3/s
1.	–90	0	0.28	0.005
2.	–75	0.083	0.32	0.007
3.	–60	0.166	0.34	0.008
4.	–45	0.249	0.47	0.01
5.	–30	0.332	0.49	0.011
6.	–15	0.415	0.53	0.013
7.	0	0.498	0.55	0.015
8.	15	0.581	0.59	0.016
9.	30	0.664	0.60	0.018
10.	45	0.747	0.63	0.019
11.	60	0.83	0.66	0.021
12.	75	0.913	0.68	0.023
13.	90	0.996	0.72	0.024

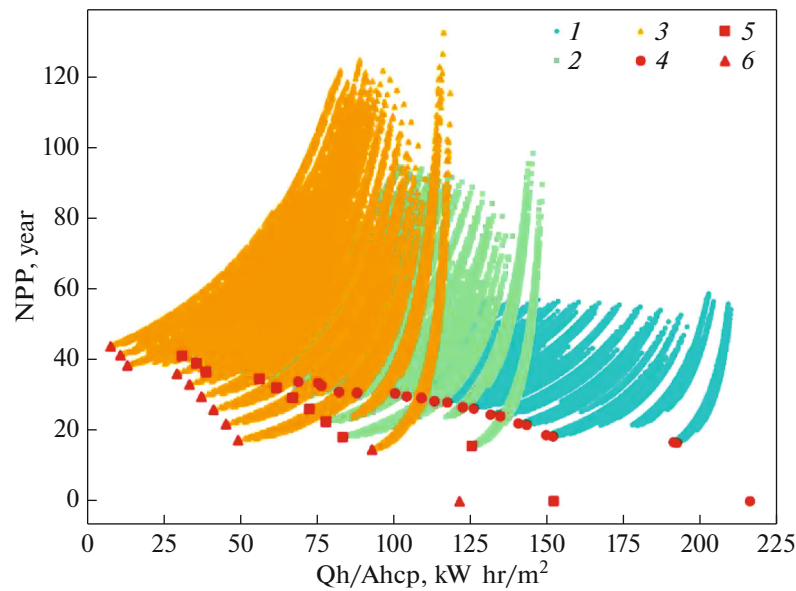


Fig. 2. Results of calculations for determining the Pareto frontiers: (1), (2), and (3), data for the first, second, and third levels of thermal protection; (4), (5), and (6), data within the Pareto frontier for the first, second, and third levels of thermal protection.

cific characteristics of the typical three-room residential building using the method of a full factorial experiment and determined the rational combinations of the experimental parameters. Pareto frontiers were

determined for the first time for the three levels of thermal protection of the typical three-room residential building under climate conditions of Tashkent (Fig. 2 and Tables 6–8).

Table 4. Values of the parameter used in the calculation

Parameter	Value
g_u	25.1 MJ/kg
HDD	2571 degree days (18°C)
n_a	0.5 h ⁻¹
F_{CO_2}	0.726
η_u	0.47
r	14%
i	10.7%
LC	30 years
v	0.85
ξ	0.85
β_h	1

The first level of thermal protection of the building within the Pareto frontier has only 21 points (Table 6). As can be seen from Table 6, data in the first line are given for the building without the Trombe wall and the specific energy consumption is 216.4 kWh/m². The values in bold in Table 6 give a rational combination of the parameters. The specific energy consumption is 184.3 kWh/m², which is 14.8% lower than the base value.

Table 7 shows calculations for the second level of thermal protection; as follows from the calculations, the specific energy consumption decreased to 117.24 kWh/m² at optimal combinations of the parameters under study (by 23.1% lower than the base values). The minimum value of the specific energy consumption for heating is 3.45 kWh/m².

Table 5. Comparison of the analytical, experimental, and design results

Months (heating period)	Total incident solar radiation on the front surface of the southern wall, MJ/month		Total heat input, MJ/month		
	E	A	E	A	D
January	4.649	4.719	1.444	1.682	1.783
February	4.967	5.216	1.360	1.700	1.905
March	5.051	5.309	1.202	1.379	1.637
November	6.100	6.265	2.073	2.411	2.34
December	4.842	5.155	1.578	1.995	1.857

E, experiment; A, analytical result; D, results of design calculations according to formula (11).

Table 6. Results of the best combination for the first level of thermal protection

Calculation procedure	Southern wall orientation, deg	Area ratio	Reduced resistance of the translucent part of the Trombe wall, ($m^2 \text{ } ^\circ\text{C}/\text{W}$)	Air flow rate through the Trombe walls, m^3/s	Investment, USD	Specific energy consumption, $\text{kWh}/(m^2 \text{ year})$	Simple payback period, year	Discounted payback period, year	Reductions in CO_2 emissions, kg/year
1	0	0	0.28	0.005	0	216.376	0	0	0
13455	0	0.083	0.59	0.024	817.836	192.435	16.405	13.554	2106.477
13520	0	0.083	0.72	0.024	865.466	191.471	16.688	13.746	2191.343
13793	0	0.249	0.59	0.024	2453.508	152.07	18.323	14.836	5658.076
13858	0	0.249	0.72	0.024	2596.397	149.899	18.756	15.119	5849.146
13962	0	0.332	0.59	0.024	3271.344	143.479	21.551	16.891	6414.018
14027	0	0.332	0.72	0.024	3461.862	140.785	21.993	17.164	6651.098
14131	0	0.415	0.59	0.024	4089.179	134.888	24.098	18.43	7169.96
14196	0	0.415	0.72	0.024	4327.328	131.67	24.533	18.686	7453.049
14300	0	0.498	0.59	0.024	4907.015	126.296	26.16	19.626	7925.902
14365	0	0.498	0.72	0.024	5192.793	122.556	26.58	19.865	8255
14469	0	0.581	0.59	0.024	5724.851	117.705	27.862	20.584	8681.844
14534	0	0.581	0.72	0.024	6058.259	113.442	28.264	20.806	9056.952
14638	0	0.664	0.59	0.024	6542.687	109.113	29.292	21.367	9437.786
14703	0	0.664	0.72	0.024	6923.724	104.327	29.674	21.574	9858.903
14807	0	0.747	0.59	0.024	7360.523	100.522	30.51	22.021	10193.73
14976	0	0.83	0.59	0.024	8178.359	88.091	30.615	22.077	11287.46
15041	0	0.83	0.72	0.024	8654.655	82.323	31.004	22.282	11794.99
17407	15	0.913	0.72	0.024	9520.121	76.58	32.703	23.167	12300.36
28496	90	0.996	0.59	0.024	9814.031	75.523	33.46	23.553	12393.31
28561	90	0.996	0.72	0.024	10385.59	68.926	33.824	23.738	12973.82

Table 7. Results of the best combination for the second level of thermal protection

Calculation procedure	Southern wall orientation, deg	Area ratio	Reduced resistance of the translucent part of the Trombe wall, ($m^2 \cdot C/W$)	Air flow rate through the Trombe walls, m^3/s	Investment, USD	Specific energy consumption, kWh/($m^2 \cdot year$)	Payback period, year	Discounted payback period, year	Reductions in CO ₂ emissions, kg/year
1	0	0	0.28	0.005	0	152.399	0	0	0
13520	0	0.083	0.72	0.024	865.466	125.603	15.51	12.938	2357.727
13858	0	0.249	0.72	0.024	2596.397	83.516	18.101	14.69	6060.85
14027	0	0.332	0.72	0.024	3461.862	78.08	22.369	17.394	6539.147
14196	0	0.415	0.72	0.024	4327.328	72.644	26.056	19.567	7017.444
14365	0	0.498	0.72	0.024	5192.793	67.208	29.272	21.356	7495.742
14534	0	0.581	0.72	0.024	6058.259	61.772	32.102	22.857	7974.039
14703	0	0.664	0.72	0.024	6923.724	56.336	34.612	24.134	8452.336
15041	0	0.83	0.72	0.024	8654.655	38.815	36.591	25.108	9994.018
15210	0	0.913	0.72	0.024	9520.121	35.642	39.157	26.331	10273.17
28561	90	0.996	0.72	0.024	10385.59	31.142	41.131	27.243	10669.18

Table 8. Results of the best combination for the third level of thermal protection

Calculation procedure	Southern wall orientation, deg	Area ratio	Reduced resistance of the translucent part of the Trombe wall ($m^2 \cdot C/W$)	Air flow rate through the Trombe walls, m^3/s	Investment, USD	Specific energy consumption, kWh/($m^2 \cdot year$)	Payback period, year	Discounted payback period, year	Reductions in CO ₂ emissions, kg/year
1	0	0	0.28	0.005	0	121.519	0	0	0
13520	0	0.083	0.72	0.024	865.466	92.992	14.569	12.279	2510.074
13858	0	0.249	0.72	0.024	2596.397	49.309	17.267	14.136	6353.6
14027	0	0.332	0.72	0.024	3461.862	45.327	21.819	17.057	6704.032
14196	0	0.415	0.72	0.024	4327.328	41.344	25.919	19.489	7054.464
14365	0	0.498	0.72	0.024	5192.793	37.361	29.631	21.55	7404.896
14534	0	0.581	0.72	0.024	6058.259	33.379	33.008	23.323	7755.328
14703	0	0.664	0.72	0.024	6923.724	29.396	36.092	24.865	8105.76
15041	0	0.83	0.72	0.024	8654.655	13.22	38.377	25.964	9529.069
15210	0	0.913	0.72	0.024	9520.121	10.959	41.351	27.344	9727.982
28561	90	0.996	0.72	0.024	10385.59	7.688	43.814	28.445	10015.81

Table 9. Regression equations for determining the specific energy consumption

Level of thermal protection	Regression equations	R^2
I	$Q_I = 239.97 - 4.89 \times 10^{-3} \times BO - 105.5 \times AR - 37.76R_{ee,sum} - 790.41q_{sw}$	0.9110
II	$Q_{II} = 181.29 - 3.1 \times 10^{-3} \times BO - 72.79AR - 39.41R_{ee,sum} - 1174.55q_{sw}$	0.8561
III	$Q_{III} = 153.35 - 2.31 \times 10^{-3} \times BO - 61.37AR - 40.86R_{ee,sum} - 1370.32q_{sw}$	0.8215

Table 8 shows calculations for the third level of thermal protection; at different combinations of the parameters under study, the specific energy consumption is 83.88 kWh/m² and the energy consumption reduction value is 31%. Analysis of Tables 6–8 shows that it is practically possible to reduce the specific energy consumption for heating from 84.9 to 97.7%.

Based on the results of the performed calculations, we obtained regression equations for the three levels of thermal protection (Table 9).

CONCLUSIONS

This study provides the results of multiobjective optimization of integration of the Trombe wall of classical type in typical residential buildings in Uzbekistan using a full factorial experiment for the first time. The following parameters were used as experimental factors: orientation of the southern wall of the typical building; thermal resistance of translucent fences of the building; ratio of the surface area of the Trombe wall to the surface area of the building facade; and air flow rate through the Trombe wall. As follows from the calculation results, the relative dominance of the factors within the studied range of factor values is in the following order: orientation, 4.56%; thermal resistance of translucent fencing, 58.21%; area ratio, 20.11%, and air flow rate through the Trombe wall, 17.12%. On average, the use of the optimal values can save from 11.1% to 93.7% of the annual specific energy consumption of the building during the heating period. The reduction in CO₂ emissions is 2106 to 12973 kg per year when coal is used during the heating period. Depending on the investment, the simple payback period ranges from 12.28 to 28.45 years. Regression equations were proposed for the three levels of thermal protection of the studied object, which makes it possible to determine the specific thermal load on heating.

ACKNOWLEDGMENTS

We thank colleagues from the Physical–Technical Institute NGO Physics–Sun, Academy of Sciences of the Republic of Uzbekistan for their constant support.

CONFLICT OF INTEREST

The authors declare that they do not have a conflict of interest.

REFERENCES

1. International Energy Agency Statistics, 2021. <https://www.iea.org/statistics/>. Accessed September 22, 2021.
2. Third National Communication of the Republic of Uzbekistan on the UN Framework Convention on Climate Change. Center for Hydrometeorological Service under the Cabinet of Ministers of the Republic of Uzbekistan, Tashkent, 2016, p. 220.
3. *Ukaz Prezidenta Respubliki Uzbekistan N UP-5577 “O dopolnitel’nykh merakh po sovershenstvovaniyu gosudarstvennogo regulirovaniya v sfere stroitel’sтва”* (Decree of the President of the Republic of Uzbekistan No. UP-5577 “On additional measures to improve state regulation in the field of construction”), Tashkent, 2018.
4. *KMK 2.01.04-2018: Construction Heat Engineering*, 2018.
5. *KMK 2.01.18-2018: Standards for Energy Consumption for Heating, Ventilation and Air Conditioning of Buildings and Structures*, 2018.
6. *ShNK 2.04.16-2018: Solar Hot Water Installations*, 2018.
7. *KMK 2.03.13-19: Floors*, 2019.
8. *KMK 2.03.10-2019: Roofs and Housetops*, 2019.
9. Pacheco, R., Ordóñez, J., and Martinez, G., Energy efficient design of building: A review, *Renewable Sustainable Energy Rev.*, 2012, vol. 16, no. 6, pp. 3559–3573.
10. Halimov, A., Nürenberg, M., Müller, D., Akhatov, J., and Iskandarov, Z., Multi-objective optimization of complex measures on supplying energy to rural residential buildings in Uzbekistan using renewable energy sources, *Appl. Sol. Energy*, 2020, vol. 56, no. 2, pp. 137–148.
11. Avezova, N.R., Avezov, R.R., Samiev, K.A., and Kakharov, S.K., Comparative heating performance and engineering economic indicators of the “Trombe wall” system in different climate zones of Uzbekistan, *Appl. Sol. Energy*, 2021, vol. 57, no. 2, pp. 128–134.
12. Harkouss, F., Fardoun, F., and Biwole, P.H., Passive design optimization of low energy buildings in different climates, *Energy*, 2018, vol. 165, pp. 591–613.
13. Duffie, J. and Beckman, W., *Solar Engineering of Thermal Processes*, New York: Wiley, 2013.
14. Morse, E.L., US Patent US246626A, 1881.

15. Trombe, F. and Michel, J., US Patent US3832992A, 1972.
16. Wang, D., Hu, L., Du, H., Liu, Y., Huang, J., Xu, Y., and Liu, J., Classification, experimental assessment, modeling methods and evaluation metrics of Trombe walls, *Renewable Sustainable Energy Rev.*, 2020, vol. 124, p. 109772.
17. Saadatian, O., Sopian, K., Lim, C.H., Asim, N., and Sulaiman, M.Y., Trombe walls: a review of opportunities and challenges in research and development, *Renewable Sustainable Energy Rev.*, 2012, vol. 16, pp. 6340–6351.
18. Duan, S., Jing, C., and Zhao, Z., Energy and exergy analysis of different Trombe walls, *Energy Build.*, 2016, vol. 126, pp. 517–523.
19. Briga Sá, A.C., Martins, A., Boaventura-Cunha, J., Carlos Lanzinha, J., and Paiva, A., An analytical approach to assess the influence of the massive wall material, thickness and ventilation system on the Trombe wall thermal performance, *J. Build. Phys.*, 2017, vol. 41, pp. 445–468.
20. Jaber, S. and Ajib, S., Optimum design of Trombe wall system in Mediterranean region, *Sol. Energy*, 2011, vol. 85, pp. 1891–1898.
21. Abbassi, F. and Dehmani, L., Experimental and numerical study on thermal performance of an unvented Trombe wall associated with internal thermal fins, *Energy Build.*, 2015, vol. 105, pp. 119–128. <https://doi.org/10.1016/j.enbuild.2015.07.042>
22. Khalifa, A.J.N. and Abbas, E.F., A comparative performance study of some thermal storage materials used for solar space heating, *Energy Build.*, 2009, vol. 41, no. 4, pp. 407–415.
23. Samiev, K.A., Simulation of thermal regime of room, heated by passive insolation solar heating systems with three-layer ventilated translucent barriers, *Appl. Sol. Energy*, 2009, vol. 45, no. 4, pp. 298–302.
24. Toiliev, K. and Annaev, K., Comparative indicators of the microclimate and heat resistance of buildings, *Izv. Akad. Nauk Turkm. SSR*, 1987, no. 3, pp. 103–105.
25. Toiliev, K. and Ashirbaev, M.Kh., Efficiency of a passive solar heating system combined with heat pipes, *Izv. Akad. Nauk Turkm. SSR*, 1987, no. 6, pp. 50–53.
26. Avezova, N.R. and Sadykov, Zh.D., Influence of the thermal resistance of the collecting-accumulating wall of a passive solar heating system on the replacement factor of heat load, *Appl. Sol. Energy*, 2012, vol. 48, no. 1, pp. 42–46.
27. Samiev, K.A., Heat efficiency of complex translucent barrier with partially absorbing layer and airway in passive solar insolation heating systems, *Appl. Sol. Energy*, 2008, vol. 44, no. 4, pp. 291–294.
28. Kreider, J.F., Curtiss, P.S., and Rabl, A., *Heating and Cooling of Buildings*, London: Taylor & Francis, 2010.
29. Malyavina, E.G., *Teplopoteri zdaniya* (Building Heat Loss), Moscow: AVOK-PRESS, 2007.
30. *ISO 13790:2008 Energy Performance of Buildings—Calculation of Energy Use for Space Heating and Cooling*, 2008.
31. Zhang, H. and Shu, H.A., Comprehensive evaluation on energy, economic and environmental performance of the Trombe wall during the heating season, *J. Therm. Sci.*, 2019, vol. 28, pp. 1141–1149.
32. Tiwari, G.N., Tiwari, A., and Shyam, *Handbook of Solar Energy. Theory, Analysis and Applications*, Singapore: Springer, 2016.
33. *GOST (State Standard) 24866-99: Glued double-glazed windows for construction purposes, Specifications*, 2000.
34. <http://okna-akfa.uz/>. Accessed October 15, 2021.
35. Montgomery, D.C., *Design and Analysis of Experiments*, Hoboken, NJ: Wiley, 2013.
36. *KMK 2.01.01-94: Climatic, Physical, and Geological Data for Design*, 1994.
37. *ShNK 2.08.01-2019: Residential Buildings*, 2020.
38. The Central Bank of the Republic of Uzbekistan. Press Releases. https://cbu.uz/ru/press_center/releases/549560/. Accessed October 15, 2021.
39. Uzbek Commodity Exchange. <https://uzex.uz/uz-Cyrl/pages/weekly-quotes>. Accessed October 15, 2021.
40. Bank.Uz. <https://bank.uz/currency/archive/15-10-2021>. Accessed October 15, 2021.
41. Ruiz-Pardo, A., Domínguez, S.A., and Fernandez, J.A.S., Revision of the Trombe wall calculation method proposed by UNE-EN ISO 13790, *Energy Build.*, 2010, vol. 42, pp. 763–773. <https://doi.org/10.1016/j.enbuild.2009.11.018>
42. Taşdemiroğlu, E. and Tinaut, D., Comparison of an analytical model with experimental results for a passive thermal storage wall, *Sol. Energy*, 1985, vol. 35, no. 3, pp. 283–286.
43. Analysis of Results of Energy Monitoring over the Heating Season of 2014–2015 after Application of Energy-Efficient Measures and Renewable Energy in a Pilot Four-Room Rural House. Promoting Energy Efficiency in Public Buildings in Uzbekistan, conducted jointly by the United Nations Development Programme (UNDP), the Global Environment Facility (GEF), and the State Committee for Architecture and Construction of the Republic of Uzbekistan, 2015.

Translated by D. Zabolotny